









Research Article

Petrographic and Geochemical Study of the Yandingui-Yangba Massif (Bafia, Central Cameroon): Geodynamic Implications

Rose No ð Ngo Belnoun¹ , Victor Metang^{1,*} , Zenon Itiga² ,
Danielle Christiane Ananga Olomo¹ , Lucien Paul Bamagalena¹ ,
Boris Tchouta Toyi¹ , Lucie Jenny Eyimi¹ , Berthol Manfo Yemkeu¹ 

¹Department of Earth Sciences, Faculty of Science, University of Yaounde I, Yaounde, Cameroon

²Department of Earth Sciences, Faculty of Science, University of Douala, Douala, Cameroon

Abstract

Several diverse models and hypotheses have been proposed to understand the dynamics of the Central African Pan-African Belt. The lack of agreement among these proposals suggests that it would be better to continue large scale mapping to provide answers to this regional issue. In this perspective, the NE-SW oriented Yandingui-Yangba rock massif, located about thirty kilometers north of Bafia, and intrudes a Precambrian metamorphic basement. The petrographic study of the massif reveals two lithological units: the metamorphic unit, which includes orthogneiss and amphibolite enclaves, and the intrusive magmatic unit, composed of amphibole-biotite granites. Geochemically, the rocks of Yandingui-Yangba ($67.85 < \text{SiO}_2 < 71.06$) are metaluminous I-type granites ($\text{A/CNK} < 1.1$), associated with the shoshonitic series and of magnesian nature ($0.67 < \text{FeOt}/(\text{MgO} + \text{FeOt}) < 0.78$). Mantle-normalized trace element spectra show a subparallel pattern between the granites and orthogneiss, indicating a common origin. These rocks were emplaced in a volcanic arc setting in a subduction-collision context. The presence of positive anomalies in U, K, Pb, and Zr, and negative anomalies in Th, Nb, and Ti, is characteristic of crustal-derived rocks. The magma that generated these granites resulted from the partial melting of metagreywackes in the lower crust, as evidenced by the low concentrations of Ni and Cr. This melting was likely facilitated by heat influx from mantle-derived magma during the Pan-African orogeny.

Keywords

Granites, Orthogneiss, Enclave, Shoshonitic, I-Type, Pan-African, Yandingui-Yangba

1. Introduction

The Precambrian basement of Cameroon (Figure 1) consists of the NW portion of the Congo Craton (Ntem and Nyong complexes) and Pan-African formations, which cover

about two-thirds of the country's surface [26, 41]. The North Equatorial Pan-African Belt (CPNE: [26] or the Central African Pan-African Belt (CPAC: [41]) formed due to the colli-

*Corresponding author: metangvictor@yahoo.fr (Victor Metang)

Received: 30 March 2025; Accepted: 15 April 2025; Published: 9 May 2025



Copyright: © The Author(s), 2025. Published by Science Publishing Group. This is an **Open Access** article, distributed under the terms of the Creative Commons Attribution 4.0 License (<http://creativecommons.org/licenses/by/4.0/>), which permits unrestricted use, distribution and reproduction in any medium, provided the original work is properly cited.

sion between the Congo-São Francisco Craton, the West African Craton, and the Saharan Metacraton [18]. In Cameroon, the Pan-African belt is divided into three domains: northern, central, and southern. These domains have been the subject of numerous studies, leading to various hypotheses and models, including: the hypothesis of an epicontinental

marine basin on a passive margin [27], a peri- or intracratonic continental basin model [42, 43, 19], the double indentation model [18], the transpressive tectonic model [7]. In the central domain, where the Yandingui-Yangba granite massif is located, Nkoumbou et al. [23] supported the hypothesis that this domain, also called Adamawa-Yadé represents a micro.

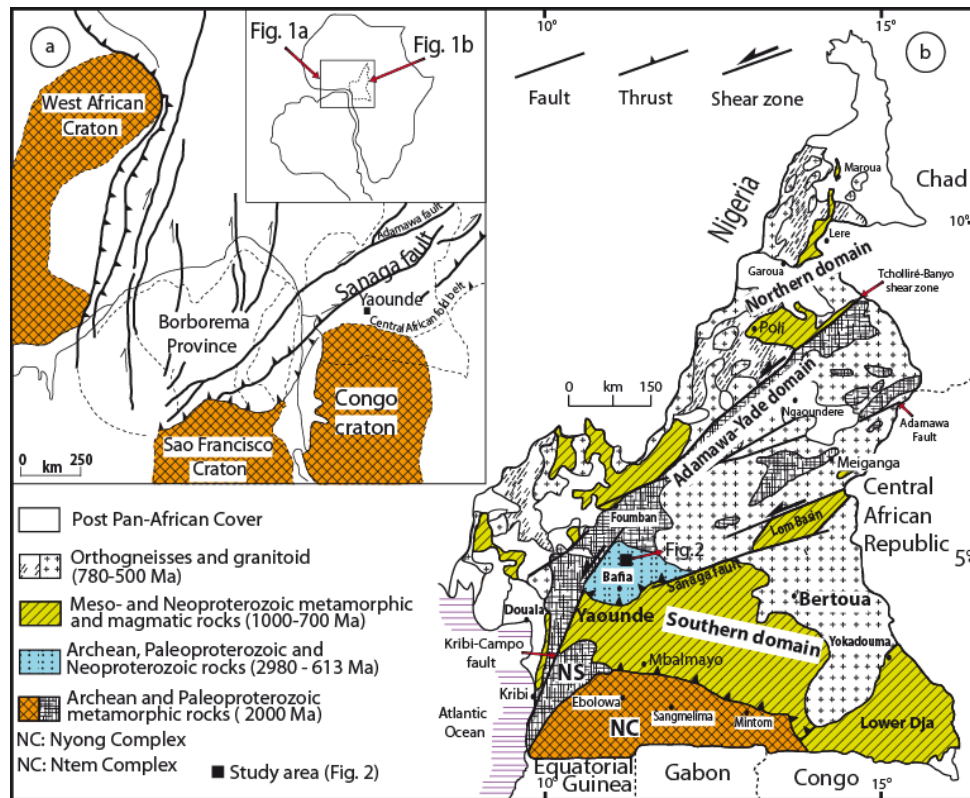


Figure 1. The Pan-African Belt of Central Africa: (a) Continent scale geodynamic reconstruction [30]; (b) Map of different lithotectonic units of Cameroon (modified from [38]).

Continent detached from the Congo Craton. Tchakounté et al. [39] proposed a model suggesting that granitoids from the Adamawa-Yadé block originated from partial melting during the northward subduction of the Yaoundé Group. These various hypotheses remain inconclusive, highlighting the need for further large-scale geological mapping to enhance our understanding of the CPNE and particularly the central domain. The main objective of this study is to map the Yandingui-Yangba massif by identifying its lithological units through petrographic and geochemical analyses. This will contribute to the broader understanding of the CPNE.

2. Geological Context

The Central Cameroon domain, which includes the study area, lies between the northern and southern domains. It is characterized by major shear zones, including: (i) the Central Cameroon Shear Zone (CCSZ), (ii) the Fouban-Tibati-Banyo Fault (FTBF), (iii) the B'ar é Oya

Fault (BOF), and (iv) the Sanaga Fault (SF). This domain is predominantly composed of syn-tectonic hyperpotassic granitoids with a calc-alkaline affinity and Pan-African age, hosted within highly metamorphosed rocks [24, 22, 29, 35]. Previous geological studies near Yandingui-Yangba include those of Wecksteen [44], which led to the small-scale geological map of East Douala. Wecksteen [44] identified gneiss, micaschists, and quartzites, along with biotite - amphibole migmatites and magmatic rocks such as amphibole - biotite granites (Figure 2). Recent studies in the Bafia area have identified Neoproterozoic formations (granitoids, metasedimentary gneiss, quartzites, garnet-biotite gneiss) and Paleoproterozoic formations (amphibolites, amphibole-bearing pyroxenites, undifferentiated gneiss) [38, 39, 20]. Gneiss, micaschists, and quartzites originate from eroded Archean and Paleoproterozoic crustal materials, including pelites, greywackes, litharenites, arkoses, and ferruginous sands [8, 36, 37]. In contrast, granitoids are characteristic of passive margin formations [8] and are associated with Pan-African-age metaplutonites [37, 38].

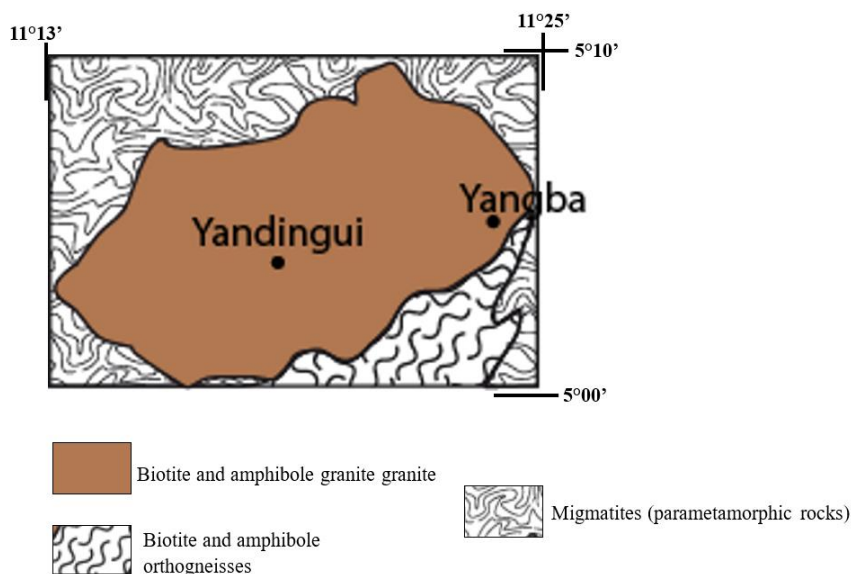


Figure 2. Geological map of Yandingui-Yangba.

These geological formations have undergone four deformation phases: D₁ phase: Characterized by S₁ schistosity, L₁ mineral lineation, and P₁ folds. It corresponds to amphibolite facies metamorphism of medium to high grade [24, 22, 29, 35, 11]. D₂ phase: Marked by C₂ shear zones, P₂ folds, S₂ schistosity, and L₂ lineaments. This phase corresponds to high-grade amphibolite facies metamorphism (5-7 kb, 700-800 °C) [24, 22, 29, 11]. D₃ phase: A transcurrent tectonic phase associated with dextral shear movements, characterized by medium-grade amphibolite facies metamorphism. D₄ phase: A brittle deformation phase responsible for the emplacement of granitic veins [11, 12].

3. Methodology

Geochemical analyses of major and trace elements were conducted at the Department of Geosciences, University of Padua, Italy. Rock samples were pulverized using an agate mortar, and glass beads were prepared after calcination and addition of lithium tetraborate (Li₂B₄O₇) in a 1:10 dilution ratio. Quantitative analyses of oxides (SiO₂, TiO₂, Al₂O₃, Fe₂O₃, MnO, MgO, CaO, Na₂O, K₂O, P₂O₅) and trace elements (Sc, V, Cr, Co, Ni, Cu, Zn, Ga, Rb, Sr, Y, Zr, Nb, Ba, La, Ce, Nd, Pb, Th, U) were performed using a Philips PW2400 spectrometer. Geological standards were used for calibration, with analytical errors ranging from 1-2% for major elements and 10-15% for trace elements.

4. Results

4.1. Petrography

An inventory of the different petrographic types present in the study area and their macroscopic and microscopic descriptions was carried out. This scientific approach identified

two lithological groups: a magmatic group consisting of biotite and amphibolite granite, and a metamorphic group consisting of orthogneiss and amphibolite. All these rocks outcrop along watercourses, on hilltops, and slopes in the form of slabs, boulders, and blocks (Figure 3a, 3b, and 3c).

4.1.1. Metamorphic Unit

(i) Orthogneiss

Orthogneiss outcrops as slabs about five kilometers northeast of Fian at an altitude of 676 m. The rock has a gray appearance and a foliated structure (Figure 3d), characterized by the alternation of ferromagnesian minerals (amphibole and biotite) and quartzofeldspathic minerals. Other outcrops are found in the localities of Beka and Banda. Under the microscope, the rock exhibits a granonematolipidoblastic heterogranular texture (Figure 3e). It consists of quartz, feldspar, green hornblende, biotite, garnet, and accessory minerals such as sphene, apatite, and opaque minerals. Quartz (30-35%) is anhedral, sometimes forming small interlocking grains located in feldspar interstices. The crystal size ranges from 0.1 mm to 1.5 mm (Figure 3f), and quartz is often included in feldspars and green hornblende. Alkaline feldspar (20-25%) consists of orthoclase blasts that are difficult to characterize due to deformation, with sizes between 0.2 mm and 3 mm (Figure 3f). Microcline (5-10%) is subhedral to anhedral, with large crystals up to 5 mm (Figure 4a), often perthitized and exhibiting exsolution textures oriented along pericline twinning. Plagioclase (5-10%) forms xenomorphic to amoeboid-shaped blasts around 0.2 mm in size, showing alteration (sericitization). Green hornblende (10-15%) occurs as xenomorphic to subhedral blasts (0.5 mm - 1.6 mm), sometimes fragmented and containing opaque mineral inclusions. Biotite (5-10%) appears as elongated subhedral flakes, sometimes reaching 1.5 mm, often included in feld-

spars and amphiboles. Spene (0.2-0.4 mm) (Figure 3f) is subhedral to euhedral and found near amphiboles. Garnet (2%) occurs in clusters of multiple individuals (Figure 4b). Opaque minerals and apatite (1%) vary in size and shape, with apatite mainly included in amphibole.

(ii) Amphibolites

Amphibolite outcrops as slabs west of Yandingui-Yangba. It has a dark gray to greenish color, consisting of white minerals such as feldspar and quartz in a ferromagnesian matrix (Figure 4c), revealing a fine-grained banded structure. Microscopically, amphibolite displays a nematogranoblastic texture (Figure 4d), primarily composed of amphibole, plagioclase, quartz, and pyroxene. Amphibole (70-75%) is uniformly distributed, occurring as elongated subhedral to anhedral crystals (0.5 - 2 mm), often associated with quartz and plagioclase. Some green hornblende grains show initial chloritization. Plagioclase (15-20%) appears as anhedral crystals (1 - 2 mm), scattered within the matrix. Quartz (3%) is rounded, sometimes included in hornblende, and varies between 0.5 and 1.5 mm. Clinopyroxene (2%) is anhedral and alters to amphibole. Accessory minerals include spene, opaque minerals, and apatite.



Figure 3. Photographs and microphotographs of granites and orthogneiss: a) outcrop in rounded shapes and blocks of granites in the Beka locality; b) panoramic view of the Yandingui massif; c) slab outcrop of orthogneiss; d) orthogneiss sample; e) Molding of white minerals by biotite; f) euhedral crystals of spene and chloritization of biotite.

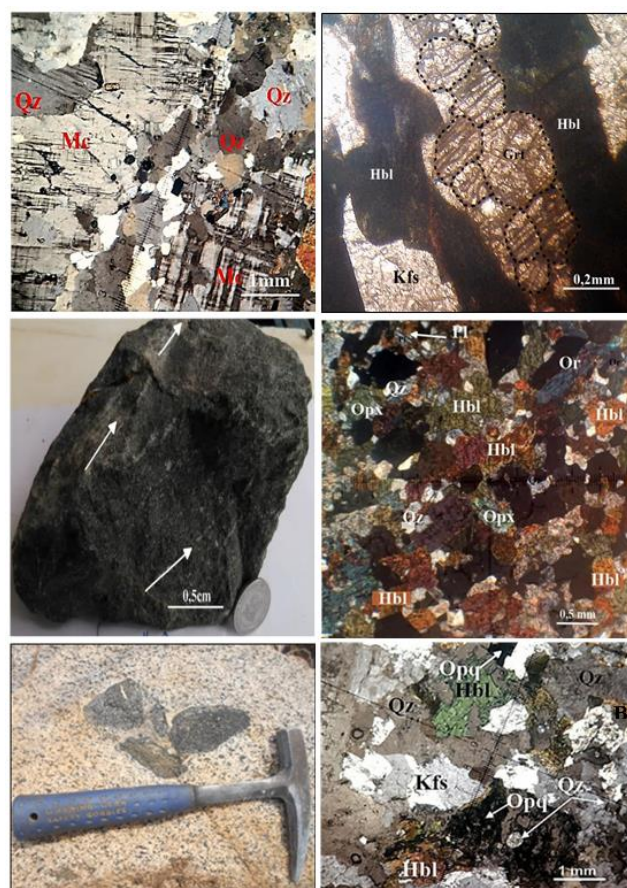


Figure 4. Microphotographs and photographs of orthogneisses, amphibolites and granites: a) microcline porphyroblasts in biotite and amphibolite orthogneisses; b) garnet aggregates parallel to green hornblende porphyroblasts; c) amphibolite sample; d) nematogranoblastic texture in amphibolites; e) outcrop of biotite and amphibolite granite with amphibolite enclaves; f) heterogranular granular texture in biotite and amphibolite granites.

4.1.2. Magmatic Unit Biotite and Amphibolite Granites

Biotite and amphibolite granites are fine- to coarse-grained (Figure 4e) and outcrop in Banda and Langba. Under the microscope, they contain quartz, feldspars (microcline, orthoclase, and plagioclase), amphibole (green hornblende), and secondary opaque minerals. The rock has a heterogranular granular texture (Figure 4f). Quartz (35-40%) occurs as anhedral crystals up to 0.2 mm, filling interstitial spaces between feldspars. Microcline (10-15%) forms subhedral megacrysts (1-2 mm), randomly oriented with perthitic lamellae. Orthoclase (5-10%) appears as subhedral crystals (0.2-0.6 mm), closely associated with quartz and plagioclase, showing pericline twinning. Plagioclase (15-20%) occurs as subhedral grains (~0.8 mm), with some automorphic grains (~0.2 mm) showing sericitization. Green hornblende (10-14%) is subhedral to euhedral, occasionally twinned, Table 1. Rock sample geochemistry of major and trace elements with larger crystals reaching 1 mm. Biotite (1%) forms fine euhedral flakes (~0.2 mm), dispersed within the rock. Opaque minerals and sericite (1%) result from am-

phibole and plagioclase alteration.

Table 1. Rock sample geochemistry of major and trace elements

	Biotite and amphibole orthogneisses			amphibolites		Biotite and amphibole granites								
	ND17	ND7	ND19	ND9	ND15	ND16	ND22	ND23	ND11	ND12	ND14	ND1	ND2	ND6
SiO ₂	69.97	64.98	69.92	49.06	70.03	71.06	67.85	70.61	70.05	73.05	77.09	71.71	71.48	70.43
TiO ₂	0.46	0.61	0.87	1.41	0.33	0.29	0.56	0.28	0.39	0.39	0.20	0.25	0.29	0.31
Al ₂ O ₃	14.84	15.35	12.34	14.01	14.33	13.93	14.09	14.97	14.69	13.08	11.48	13.61	13.59	13.79
Fe ₂ O ₃	3.00	5.40	6.59	13.34	2.42	2.17	3.83	2.17	2.72	2.11	1.88	2.03	2.73	2.55
MnO	0.05	0.13	0.12	0.22	0.05	0.05	0.08	0.03	0.07	0.05	0.01	0.06	0.06	0.06
MgO	1.29	2.22	0.55	7.39	0.59	0.47	1.10	0.52	0.90	0.63	0.02	0.36	0.44	0.62
CaO	3.20	3.81	2.77	10.62	1.45	1.28	2.20	1.71	1.52	1.59	0.43	1.72	1.19	1.57
Na ₂ O	4.12	4.95	2.20	2.33	3.88	3.44	3.35	3.65	4.03	3.34	2.98	2.72	3.24	3.17
K ₂ O	2.17	1.58	4.17	0.78	6.16	6.63	6.41	5.51	5.12	4.68	5.16	7.20	6.59	6.91
P ₂ O ₅	0.11	0.16	0.23	0.13	0.08	0.07	0.14	0.11	0.10	0.15	0.01	0.06	0.07	0.08
Tot	99.21	99.19	99.76	99.29	99.32	99.39	99.61	99.56	99.59	99.07	99.26	99.72	99.68	99.49
L.O.I.	1.66	0.78	0.56	1.18	0.45	0.50	0.42	0.72	1.73	0.43	0.30	0.87	0.61	0.51
S	339	51	58	63	22	11	28	28	20	36	<10	53	21	27
Sc	<5	<5	25	26	<5	12	12	<5	10	9	9	8	12	6
V	37	72	14	284	23	15	40	30	31	29	<5	17	25	24
Cr	30	24	<6	171	<6	<6	15	<6	14	<6	<6	<6	17	<6
Co	55	152	154	91	126	231	162	144	199	205	236	170	211	144
Ni	14	21	3	70	8	6	14	<3	10	<3	<3	5	10	11
Cu	53	59	32	83	42	15	25	26	31	19	22	19	22	19
Zn	40	86	118	116	39	25	61	20	42	29	94	15	37	36
Ga	24	31	26	24	23	22	25	23	23	22	25	20	23	23
Rb	53	105	135	20	113	127	174	128	155	136	130	206	152	166
Sr	470	519	162	348	623	619	771	742	461	347	28	542	622	611
Y	14	17	85	31	18	14	22	9	24	24	43	19	21	20
Zr	146	122	454	71	183	179	242	104	163	184	363	163	193	181
Nb	4	9	28	5	8	7	13	3	11	15	8	10	8	8
Ba	964	370	1325	286	2536	2547	2764	2191	1826	782	332	2786	2840	2857
La	33	28	99	<10	19	23	22	<10	16	24	45	17	20	25
Ce	65	66	209	<10	81	95	104	65	105	100	84	85	103	87
Nd	<10	26	25	16	<10	<10	<10	<10	<10	<10	33	<10	<10	<10
Pb	29	31	32	17	47	40	47	52	52	40	36	54	45	49
Th	5	9	13	3	<3	<3	<3	<3	4	8	9	<3	<3	<3
U	3	8	7	4	9	7	7	9	8	10	11	9	11	12

4.2. Geochemistry

4.2.1. Major Elements

The rocks studied exhibit a rather homogeneous chemical composition in major elements (Table 1) in biotite and amphibolite orthogneisses (64.98-69.97), amphibolites (49.6), and biotite and amphibolite granites (67.85-77.09). The A/CNK ratio ranges from 1.02 to 1.56, thus reflecting the aluminous nature of these rocks. The SiO_2 content ranges from 64.98 to 69.97% in the orthogneisses, 49.06% in the amphibolites, and 65.87 to 77.09% in biotite and amphibolite granites. The sum of the elements associated with ferromagnesian minerals ($\text{Fe}_2\text{O}_3 + \text{MgO} + \text{TiO}_2$) ranges from 4.75 to 8.23% in the orthogneisses, 22.14% in the amphibolites, and 2.97 to 5.49% in the amphibole and garnet granites. This wide variation in elements associated with ferromagnesian miner-

als not only explains the diversity of lithological units but also the existence of several petrographic facies within the biotite and amphibolite granites. The CaO content (2.77-3.81% in the orthogneisses, 10.62% in the amphibolites, and 0.43-1.72% in the biotite and amphibolite granites) and TiO_2 content (0.46-0.87% in the orthogneisses, 1.41% in the amphibolites, and 0.2 to 0.56% in the biotite and amphibolite granites) are also variable and reflect, in some cases, the richness in plagioclase and titaniferous minerals.

The Harker diagrams (Figure 5) show that certain chemical elements such as Al_2O_3 , CaO, MgO, Fe_2O_3 , TiO_2 , P_2O_5 , and Na₂O in the granites and orthogneisses have negative correlations with SiO_2 . A positive correlation is observed with K_2O . A slight dispersion of points is observed with P_2O_5 and K_2O . Overall, the P_2O_5 content decreases with silica, while the K_2O content increases.

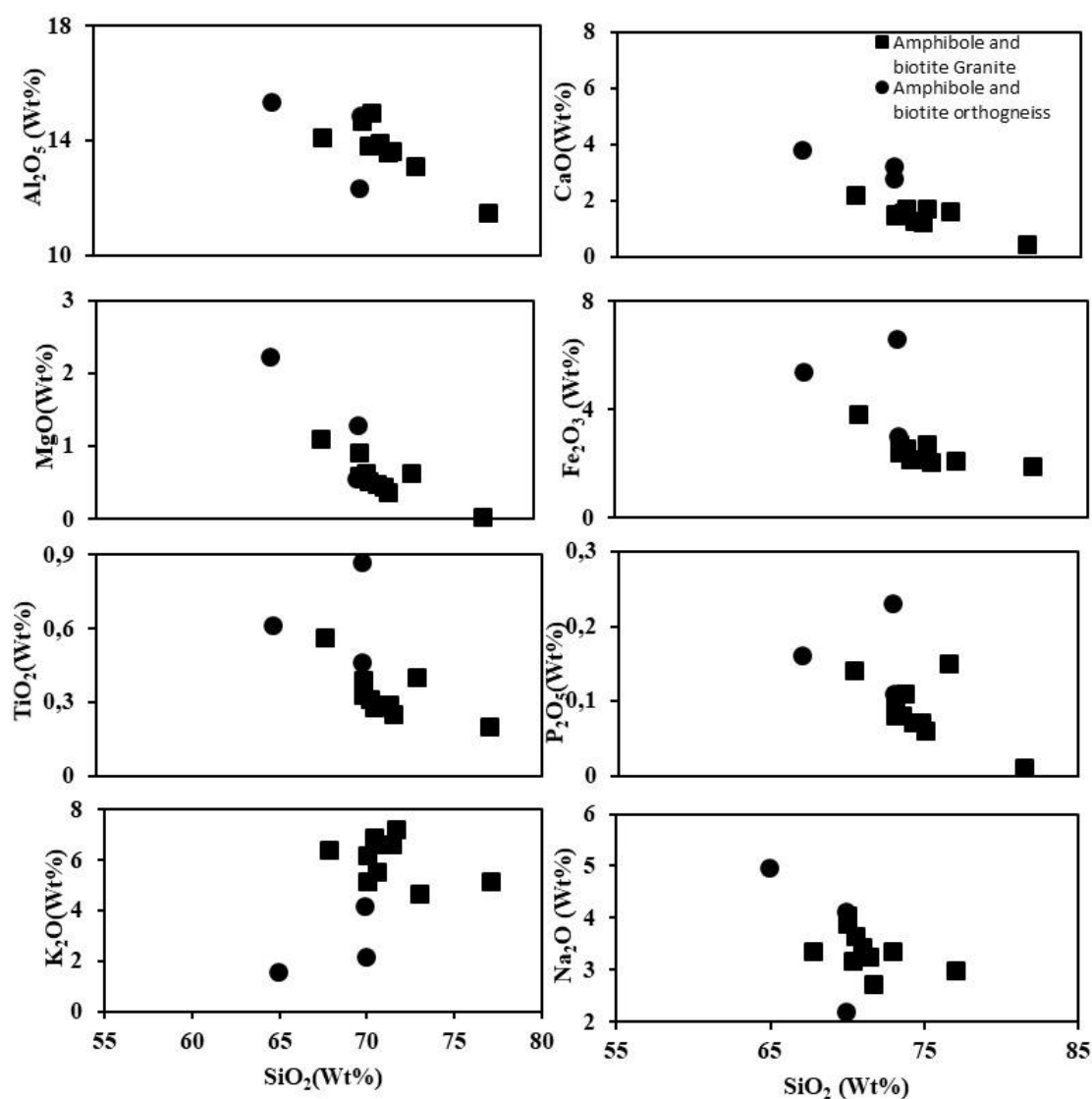


Figure 5. Harker type variation diagram for major elements as a function of SiO_2 (% by weight).

4.2.2. Nomenclature and Classification of Rocks

The geochemical data plotted in the TAS (Total Alkali Silica) diagram of Cox et al. [3] in Figure 6 show that of the ten samples of amphibole-biotite granites, nine fall within the granite domain and one within the syenite domain. Two orthogneiss samples fall within the granodiorite domain, while one sample is at the intersection between diorites and granodiorites. The only amphibolite sample analyzed falls within the sub-alkaline gabbro field. The rocks from the Yandingui-Yangba sector range from the alkaline domain (amphibole and biotite granite) to the sub-alkaline domain (amphibolites and orthogneiss) according to the Miyashiro [17] diagram (Figure 6). These are Type-I granites according to Chappell and White [2], metaluminous, in agreement with Maniar and Piccoli [15], with $0.82 < [Al_2O_3 / (CaO + Na_2O + K_2O)] < 1.1$ (Figure 7). A few samples are located between the peraluminous and metaluminous domains (Figure 7). These samples have an A/CNK ratio between 0.99 and 1.1.

4.2.3. Series and Nature of Rocks in the Study Area

The Yandingui-Yangba granites belong to the shoshonitic series, as indicated by the Peccerillo and Taylor [32] diagram in Figure 8, while the orthogneisses range from the calc-alkaline series to the medium to very K-rich series. The $FeOt/(FeOt + MgO)$ vs. SiO_2 diagram of Frost et al. [6] in Figure 9 shows that the granites and amphibolites are generally magnesian in nature, while the orthogneisses are ferro-magnesian in nature.

4.2.4. Geotectonic Context

The Pearce et al. [31] diagrams show that the Yandin gui-Yangba granites occupy the volcanic arc granite domain in a syn-collisional context (Figure 10), while the orthogneisses are distributed between the intraplate granite domain and the volcanic arc granite domain in a syn-collisional context.

4.2.5. Trace Elements

The trace element spectra in Figure 11a, obtained by normalizing to the primitive mantle of Sun and McDonough [34], show that the granites of Yandingui-Yangba exhibit positive anomalies in U, Pb, Ba, K, Pb, and Sr (except for sample D14) and negative anomalies in Th, Nb, La, Nd, and Ti. The spectra of the orthogneiss (Figure 11b) show positive anomalies in U and Pb and negative anomalies in Nb and Ti. The Harker diagrams (Figure 12) of the trace elements (ppm) in Figure 11 display varied chemical behavior observed in amphibole and biotite granites as well as in amphibole and biotite orthogneiss. Negative correlations are observed between SiO_2 and Ba, and U, while positive correlations exist between SiO_2 , Ga, and Zn. These diagrams also show dispersions between SiO_2 and Rb, Nb, and Zr.

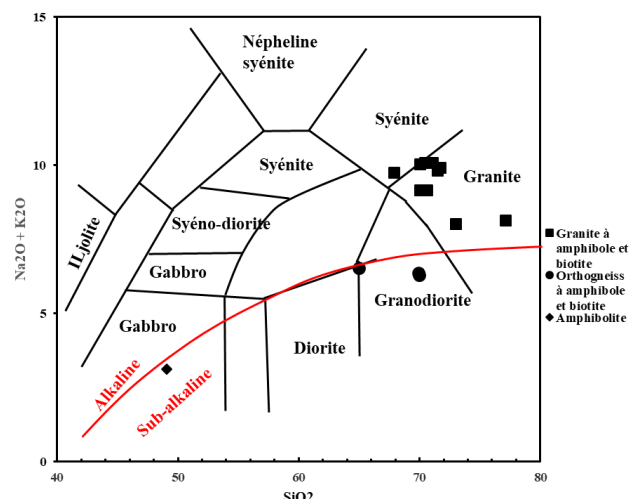


Figure 6. Nomenclature and geochemical classification of Yandin-gui-Yangba granites: TAS diagram by Cox et al. [3]; the red line marks the boundary between the alkaline and sub-alkaline domains according to Miyashiro [17].

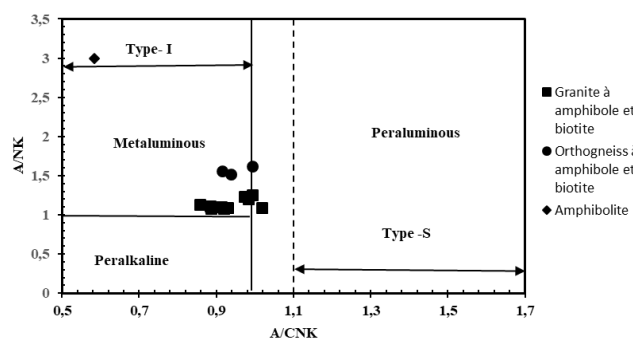


Figure 7. A/NK $[Al_2O_3 / (Na_2O + K_2O)]$ vs. A/CNK $[Al_2O_3 / (CaO + Na_2O + K_2O)]$ diagram according to Maniar and Piccoli [15]; the dashed line represents the boundary between Type-I granites and Type-S granites according to Chappell and White [2].

5. Discussion

5.1. Geochemistry

The superposition of the trace element spectra of granites with those of the orthogneiss from Yandingui-Yangba reveals subparallel and similar profiles (Figure 13). This suggests that these rocks may originate from the same magmatic source. The presence of positive anomalies in U, K, Pb, Zr, and negative anomalies in Th, Nb, and Ti is a characteristic of crustal-origin rocks [11]. The Yandin-gui-Yangba granites occupy the metaluminous domain in the A/NK vs. A/CNK diagram (Figure 7) with an A/CNK ratio < 1.1 , indicating that they correspond to I-type granites according to Chappell and White [2]. This geochemical signature in the intrusive granite field is confirmed by the relative abundance of amphibole and biotite in the studied

rocks. The richness of the granitoids in the study area in incompatible and particularly lithophile elements (Ba, Sr, and Rb) and their depletion in HFSE (High Field Strength Elements, Th, Ti, and Nb) (Table 1) confirm a crustal source contribution to their genesis (Pearce et al., 1984). Negative correlations between SiO_2 and Al_2O_3 , CaO , MgO , Fe_2O_3 , TiO_2 , P_2O_5 , and Na_2O (Figure 5) suggest that mineral crystallization, such as biotite, influenced the differentiation of the Yandingui-Yangba granite. Slight dispersions of K_2O , Rb, Sr, and Nb (Figures 5 and 12) are likely due to post-magmatic disturbance [11]. The decrease in MgO and CaO (Figure 5) relative to the increase in SiO_2 in the Harker diagrams indicates that hornblende fractionation played a significant role during at least an early stage of magma evolution. Additionally, the decline in Ti, Zr, and P_2O_5 reveals that, during fractionation, the separation of oxidized minerals such as iron, titanium, zircon, and apatite controlled the variation of these elements [4]. The variability in geochemical behavior (Figures 5, 11, and 12) suggests that fractional crystallization may have occurred during the evolution of the source magma, from its melting in the lower crust to its emplacement and solidification in the upper crust [35]. The characteristics linked to the calc-alkaline to shoshonitic affinities and the negative anomalies in HFSE (Nb, Th, and Ti) and positive anomalies in LILE of the Yandingui-Yangba rocks are similar to those of syn-tectonic Pan-African granitoids ([14, 12]), emplaced in a subduction-collision context ([4, 21, 16, 40]).

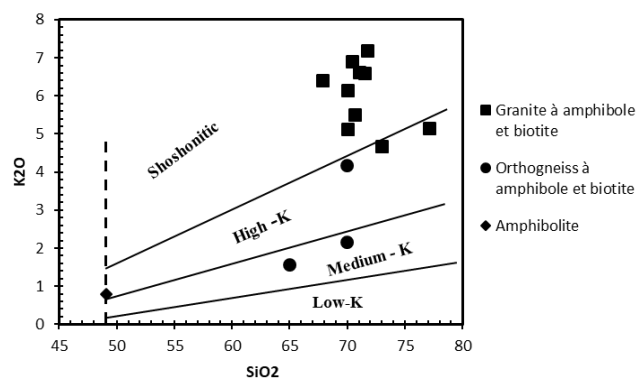


Figure 8. Peccerillo and Taylor [32] diagram.

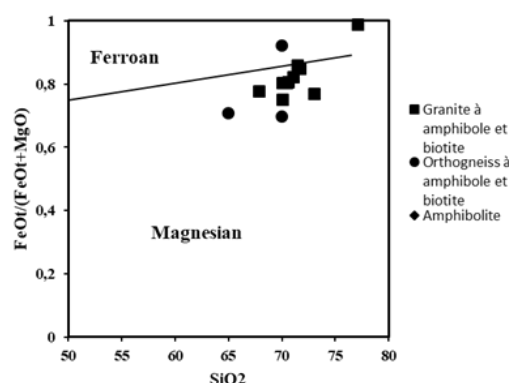


Figure 9. $\text{FeOt}/(\text{FeOt} + \text{MgO})$ vs SiO_2 diagram by Frost et al. [6], showing the magnesian affinity of granites and the magnesian-ferrous affinity of Nyandingui-Yangba orthogneiss.

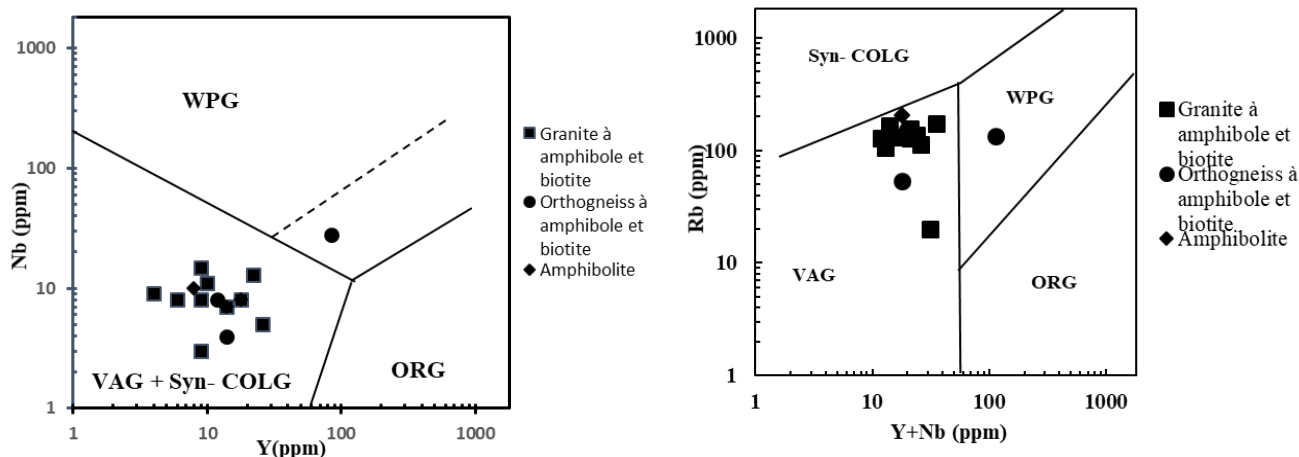


Figure 10. Geotectonic discrimination diagrams by Pearce et al. [31]: a) $\text{Rb}/(\text{Y} + \text{Nb})$ (ppm) diagram; b) Nb/Y (ppm) diagram. WPG: within-plate granites, ORG: ocean ridge granites, VAG: volcanic arc granites, Syn-COLG: syn-collisional granites.

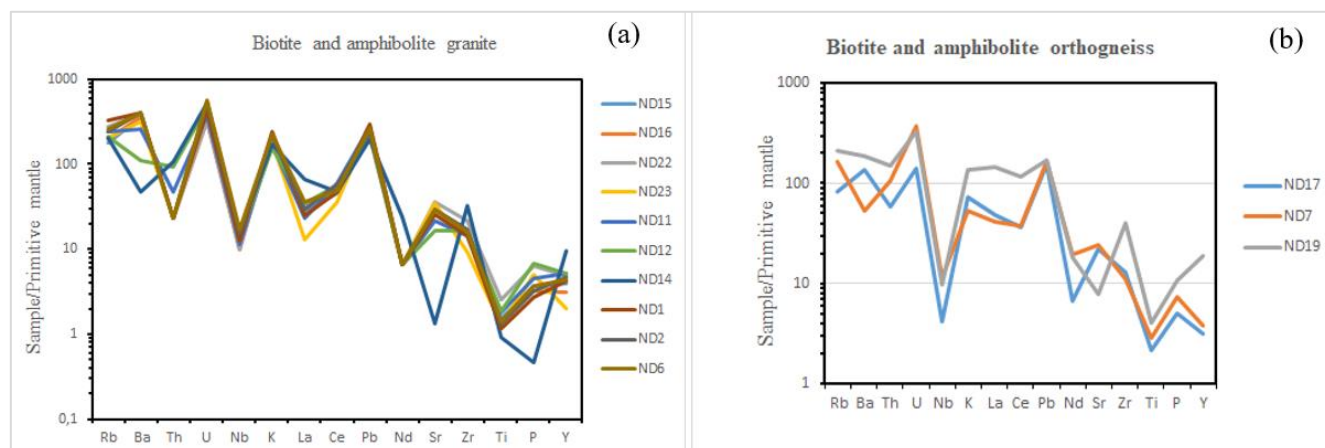


Figure 11. Trace element patterns normalized to the primitive mantle of McDonough and Sun [34]: a) Trace element patterns for Yandingui-Yangba granites; b) Trace element patterns for Yandingui-Yangba orthogneiss.

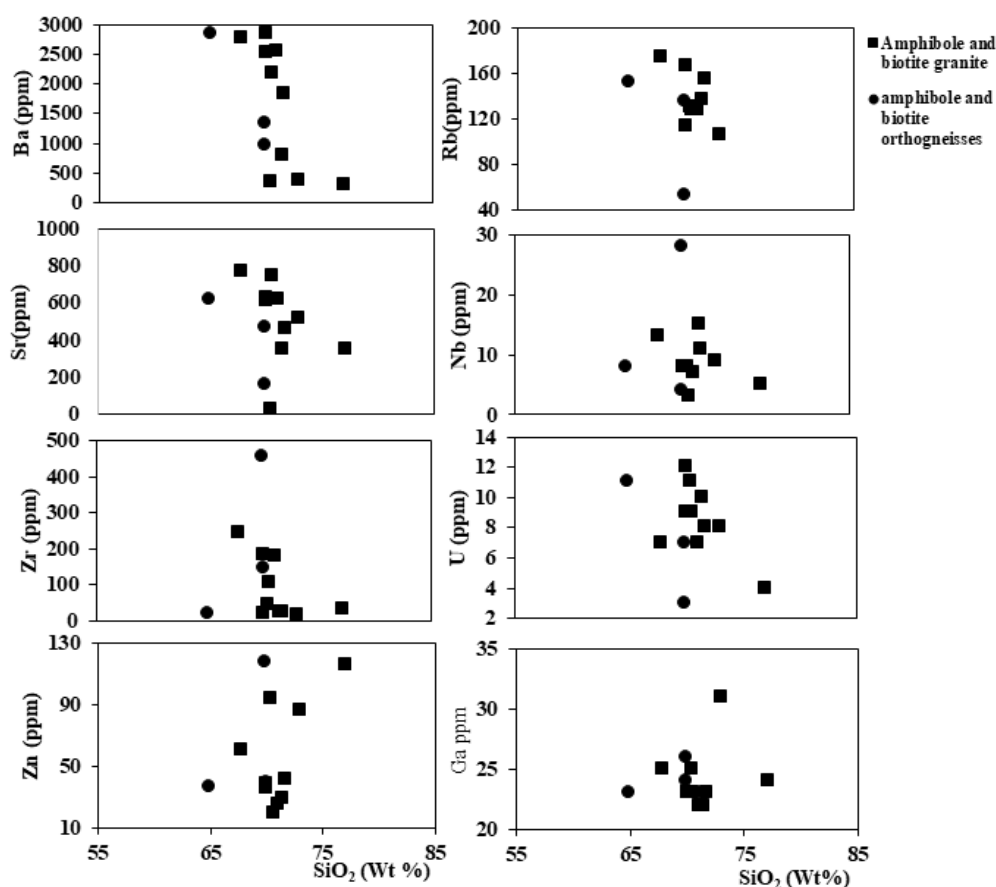


Figure 12. Harker type variation diagram for some trace elements as a function of SiO_2 .

The shoshonitic affinity of the granites may be inherited from the partial melting of older meta-igneous rocks in the lower crust [11]. Additional evidence includes low $\text{Nb} \leq 29$ contents and a strong negative Nb anomaly (Figure 13), which are typical of magmatic sources affected by subduction or lithospheric delamination according to Kay and Mahlborgkay [9] and Tchouankou é et al. [39]. This lithospheric delamination process has been proposed to explain the genesis of potassium-rich calc-alkaline and shoshonitic magmas [13, 12,

10]. In Western Cameroon, the shoshonitic affinity identified in various granitoid massifs (Fomop éa, Dschang, Bangangt é and Bafoussam) is associated with the post-collisional phase of orogeny. This shoshonitic affinity is linked to the final stage of the Pan-African orogeny [4]. The magnesian nature (Figure 9) of the Yandingui-Yangba granites is often characteristic of island arc magmas that follow oxidation and differentiation trends with low iron enrichment [5, 33].

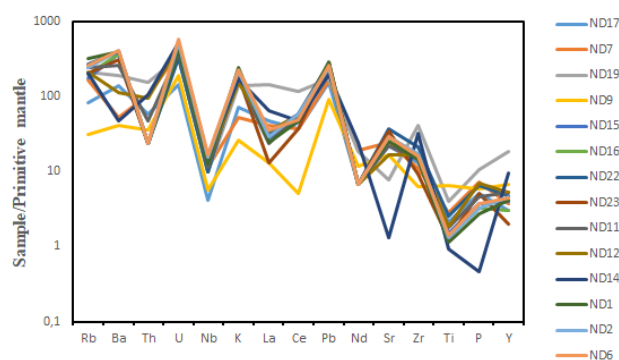


Figure 13. Trace element patterns of Yandingui-Yangba granites and orthogneiss, normalized to the primitive mantle of McDonough and Sun [34].

5.2. Magma Origin

The molar $\text{CaO}/(\text{MgO} + \text{FeOt}) / \text{Al}_2\text{O}_3/(\text{MgO} + \text{FeOt})$ diagram of Altherr et al. [1] suggests that the magmas from which these granites originated were generally derived from the partial melting of metagreywackes (Figure 14). However, one orthogneiss sample and one amphibolite sample were derived from the partial melting of metapelites. The relative abundance of hydrated minerals (amphibole and biotite) in these rocks suggests that the melting of the protoliths occurred under different hydration conditions [25]. The magmatism of the plutonic rocks of Yandingui-Yangba could thus have involved the melting of protoliths composed of metapelites and metagreywackes in the lower crust, as evidenced by their low Ni and Cr contents (Table 1). This melting would have been facilitated by the heat increase from the magma originating in the upper mantle during the Pan-African orogeny [25, 28]. This process would have occurred during the syn- to post-collisional period in the lower crust [4]. The nature of the protolith of the Yandingui-Yangba granites is similar to that obtained by Tagne-Kamga [35] in the Ngondo complex and by Nzenti et al. [25, 28] in the Akum massif.

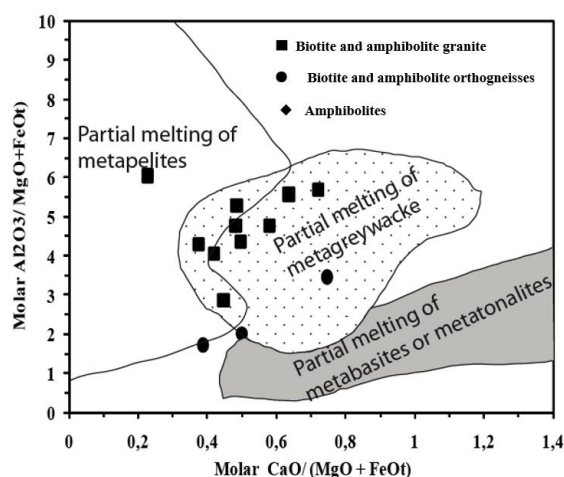


Figure 14. Molar diagram $\text{CaO}/(\text{MgO} + \text{FeOt}) / \text{Al}_2\text{O}_3/(\text{MgO} + \text{FeOt})$ by Altherr et al. (2000).

6. Conclusion

The Yandingui-Yangba granite massif contains numerous rocks whose petrographic and geochemical studies have been initiated as part of this work. Petrographically, the study area exhibits a heterogeneous lithology composed of two petrographic units: the metamorphic unit consisting of orthogneiss and amphibolite, and the intrusive magmatic unit made up of amphibole and biotite granites. The amphibolites appear as enclaves within the amphibole and biotite granites. Regarding mineralogy, these rocks are mainly composed of alkali feldspars, quartz, plagioclase, amphibole, biotite, and occasionally opaque minerals, apatite, and zircon. These minerals display microstructures such as myrmekites, kink bands (plagioclase), proto-mylonitic micro-textures, lenticular forms (plagioclase and quartz), and chemical transformation reactions such as sericitization (plagioclase) and kaolinization (alkali feldspars). From a geochemical perspective, the Yandingui-Yangba rock massif consists of Type I, metaluminous granites ($A/\text{ACK} < 1.1$), related to the shoshonitic series and of magnesian nature. These rocks formed in a volcanic arc environment within a syn-to-post-collisional context. They exhibit relatively homogeneous concentrations of major and trace elements, and the magma responsible for their formation likely resulted from the partial melting of metagraywackes in the lower crust, characterized by low Ni and Cr contents. This melting was facilitated by heat from the magma derived from the upper mantle during the Pan-African orogeny. The trace element spectra normalized to the primitive mantle suggest that the magma that formed the rocks of Yandingui-Yangba and some granitoids from central and western Cameroon share a common origin.

Abbreviations

$A/\text{CNK} = \text{Al}_2\text{O}_3 / (\text{CaO} + \text{NaO} + \text{K}_2\text{O})$

Author Contributions

Rose Nođ Ngo Belnoun: Conceptualization, Formal Analysis, Funding acquisition, Investigation, Methodology, Resources, Supervision, Validation, Writing – original draft, Writing – review & editing

Victor Metang: Conceptualization, Funding acquisition, Investigation, Methodology, Resources, Writing – original draft, Writing – review & editing

Zenon Itiga: Conceptualization, Funding acquisition, Investigation, Methodology, Supervision, Validation, Writing – original draft, Writing – review & editing

Danielle Christiane Ananga Olomo: Investigation, Project administration, Writing – original draft

Lucien Paul Bamagalena: Funding acquisition, Investigation

Lucie Jenny Eyimi: Funding acquisition, Investigation

Berthol Manfo Yemkeu: Funding acquisition, Investigation

Conflicts of Interest

The authors declare no conflicts of interest.

References

- [1] Altherr, F. F., Holl, A., Hegner, E., Langer, C., Kreuzer, H., 2000. High-potassium, calc-alkaline I-type plutonism in the European variscides: Northern Vosges (France) and northern Schwarzwald (Germany). *Lithos* 50, pp. 51-73. [https://doi.org/10.1016/S0024-4937\(99\)00084-0](https://doi.org/10.1016/S0024-4937(99)00084-0)
- [2] Chappell, B. W., White, A. J. R., 1992. I- and S-type granites in the Lachlan Fold Belt: Transactions of the Royal Society of Edinburgh. *Earth Sciences* 83, pp. 1-12. <https://doi.org/10.1017/S0263593300005016>
- [3] Cox, K. G., Bell, J. D., Pankhurst, R. J., 1979. The Interpretation of Igneous Rocks. Georges, Allen and Unwin, London, p. 450.
- [4] Djouka, F., Schul, B., Schussler, U., Tchouankoué J. P., Nzo-lang, C., 2008. Geochemistry of the Bafoussam Pan-African I- and S-type granitoids in western Cameroon. *Journal of African Earth Sciences* 50, pp. 148-167. <https://doi.org/10.1016/j.jafrearsci.2007.11.001>
- [5] Frost, C. D., O' Nions, R. K., 1985. Caledonian magma genesis and crustal recycling. *Journal of Petrology* 26, pp. 515-544. <https://doi.org/10.1093/petrology/26.3.515>
- [6] Frost, B. R., Barnes, C. G., Collins, W. J., Arculus, R. J., Ellis, D. J., Frost, C. D., 2001. A geochemical classification for granitic Rocks. *J. Petrol.* 42, 2033-2048. <https://doi.org/10.1093/petrology/42.11.2033>
- [7] Ganno, S., Nzenti, J-P., Ngnoué T., Kankeu B., Kouankap Nono, G. D., 2010. Polyphase deformation and evidence for transpressive tectonics in the Kimbi area, Northwestern Cameroon Pan-African Fold Belt. *Journal of Geology and Mining Research* 4 (2), 1-15.
- [8] Ganwa, A. A., 1998. Contribution à l'étude géologique de la région de Kombé II-Mayabo dans la Saïe de Bafia: géomorphologie structurale, tectonique, pétrologie. Thèse Université de Yaoundé I, 193 p.
- [9] Kay, R. W., Mahlburgkay, S., 1991. Creation and destruction of lower continental crust. *International Journal of Earth Sciences* 80, pp 259-278. <https://doi.org/10.1007/BF01240068>
- [10] Kwékam, M., Affaton, P., Bruguier, O., Liégeois, J. P., Hartmann, G., & Njonfang, E., 2013. The Pan-African Kekem gabbro-norite (West-Cameroon), U-Pb zircon age, geochemistry and Sr-Nd isotopes: Geodynamical implication for the evolution of the Central African fold belt. *Journal of African Earth Sciences* 84, 70-88. <https://doi.org/10.1016/j.jafrearsci.2013.05.001>
- [11] Kwékam, M., Hartmann, G., Njanko, T., Tcheumenak Kouéno, J., Fozing, E. M., Njonfang, E., 2015. Geochemical and isotope Sr-Nd character of Dschang biotite granite: implications for the Pan-African continental crust evolution in West-Cameroon (Central Africa). *Journal of African Earth Sciences* 4, 88-102.
- [12] Kwékam, M., Liégeois, J. P., Njonfang, E., Affaton, P., Hartmann, G., Tchoua, F., 2010. Nature, origin and significance of the Fomopé Pan-African high-K calc-alkaline plutonic complex in the Central African fold belt (Cameroon). *Journal of African Earth Sciences* 54, 79-95. <https://doi.org/10.1016/j.jafrearsci.2009.11.001>
- [13] Liégeois, J. P., Abdelsalam, M. G., Ennih, N., Ouabadi, A., 2013. Metacraton: Nature, genesis and behavior. *Gondwana Research* 23, 220-237. <https://doi.org/10.1016/j.gr.2012.05.004>
- [14] Liégeois, J. P., Navez, J., Hertogen, J., Black, R., 1998. Contrasting origin of post-collisional high-K calc-alkaline and shoshonitic versus alkaline and peralkaline granitoids. The use of sliding normalization, *Lithos* 45, 1-28. [https://doi.org/10.1016/S0024-4937\(98\)00005-6](https://doi.org/10.1016/S0024-4937(98)00005-6)
- [15] Maniar, P. D., Piccoli P. M., 1989. Tectonic discrimination of granitoids. *Geological society of America Bulletin* 101, 635-643. [https://doi.org/10.1130/0016-7606\(1989\)101<0635:TDOG>2.3.CO;2](https://doi.org/10.1130/0016-7606(1989)101<0635:TDOG>2.3.CO;2)
- [16] Mbassa, J. B., Kamgang, P., Njonfang, M. E., Zenon, Itiga, B., Duchene, S., Bessong, M., Wonkwenmendang Nguet, P., Ntepe Nfomou., 2016. Evidence of heterogeneous crustal origin for the Pan-African Mbengwi granitoids and the associated mafic intrusions (northwestern Cameroon, central Africa). *Comptes Rendus Geosciences* 348, 116-126. <https://doi.org/10.1016/j.crte.2015.12.004>
- [17] Miyashiro, A., 1978. Nature of Alkaline Volcanic Rock Series. *Contribution to Mineralogy and Petrology* 66, 91-104. <https://doi.org/10.1007/BF00371327>
- [18] Ngako, V., Affaton, P., Njonfang, E., 2008. Pan-African tectonics in northwestern Cameroon: implication for the history of western Gondwana. *Gondwana Research* 14: 509-522. <https://doi.org/10.1016/j.gr.2008.02.001>
- [19] Ngako, V., Njonfang, E., 2011. Plates Amalgamation and Plate Destruction, the Western Gondwana History. Tectonics. Dr. Damien Closson (Ed.), ISBN 978-953-307-545-7, InTech. <https://doi.org/10.5772/18185>
- [20] Ngamy Kamwa, A., Tchakounte Numbem, J., Nkoumbou, C., Owona, S., Tchouankoué, J. P., Mvondo Ondo, J., 2019. Petrology and geochemistry of the Yoro-Yangben Pan-African granitoids intrusion in the Archean Adamawa-Yade crust (Sw-Bafia, Cameroon). *Journal of African Earth Sciences* 150, 401-414. <https://doi.org/10.1016/j.jafrearsci.2018.11.004>
- [21] Ngo Belnoun, R. N., Tchouankoué J. P., Zenon Itiga., Simeni Wambo N. A., Owona S., Koller F., Thäni, M., 2013. Geochemistry of the bayon plutonic complex -western Cameroon. *Global Journal of Geological Sciences* 11, pp. 73-93.
- [22] Njanko, T., 1999. Les Granitoïdes calco-alcalins syn-cisaillement de la région de Tibati (domaine Centre de la Chaîne Panafricaine): leur signification géodynamique par rapport à la tectonique Panafricaine. Thèse Doctorat 3^{ème} cycle, Université de Yaoundé I, 158 p.

- [23] Nkoubou, C., Barbey, P., Yonta-Ngouné C., Paquette, J. L., Villiéras, F., 2014. Precollisional geodynamic context of the southern margin of the Pan-African fold belt in Cameroon. *Journal of African Earth Sciences* 99: 245-260. <https://doi.org/10.1016/j.jafrearsci.2014.03.00>
- [24] Nzenti, J. P., 1998. L'Adamaoua Panafricain (région de Banyo) : une zone clé pour un modèle de la Chaîne Panafricaine Nord-Équatoriale au Cameroun. Thèse Doctorat d'État, Université Cheikh Anta Diop-Université de Nancy I, 176 p.
- [25] Nzenti, J. P., Abaga, B., Suh, C. E., Nzolang, C. 2010. Petrogenesis of peraluminous magmas from the Akum-Bamenda Massif, Pan-African Fold Belt, Cameroon. *International Geology Review*, pp. 1- 29. <https://doi.org/10.1080/00206810903442402>
- [26] Nzenti, J. P., Barbey, P., Bertrand, J. M. I., Macaudière, J., 1994. La Chaîne Panafricaine au Cameroun : cherchons suture et modèle Sociétés Géologiques de France 15, réunion des Sciences de la Terre, Nancy, France, 99 p.
- [27] Nzenti, J. P., Barbey, P., Macaudière, J., Soba, D., 1988. Origin and evolution of late Precambrian high-grade Yaoundé gneisses (Cameroon). *Precambrian Research* 38, pp. 91-109. [https://doi.org/10.1016/0301-9268\(88\)90086-1](https://doi.org/10.1016/0301-9268(88)90086-1)
- [28] Nzenti, J. P., Barbara, Abaga., Suh, C. E., Nzolang, C., 2011 : Petrogenesis of peraluminous magmas from the Akum-Bamenda Massif, Pan-African Fold Belt, Cameroon. *International Geology Review* 53, pp 1121-1149. <https://doi.org/10.1080/00206810903442402>
- [29] Nzolang, C., Kagami, H., Nzenti, J. P., Holtz, F., 2003. Geochemistry and preliminary Sr-Nd isotopic data on the Neoproterozoic granitoids from the Bantou area, West Cameroon: evidence for a derivation from a Paleoproterozoic to Archean crust. *Polar Geoscience Tokyo* 16, 196-226.
- [30] Oliveira, E. P., Toteu, S. F., Araújo, M. N. C., Carvalho, M. J., Nascimento, R. S., Bueno, J. F., McNaughton, N., Basilici, G., 2006. Geologic correlation between the Neoproterozoic Sergipano Belt (NE Brazil) and the Yaoundé Belt (Cameroon, Africa). *Journal of African Earth Sciences* 44, 470-478. <https://doi.org/10.1016/j.jafrearsci.2005.11.014>
- [31] Pearce, J. A., Harris, N. B. W., Tindle, A. G., 1984. Trace elements discrimination diagrams for the geotectonic interpretation of granite rocks. *Journal of petrology* 25, 956-983. <https://doi.org/10.1093/petrology/25.4.956>
- [32] Peccerillo, A., Taylor, S. R., 1976. Geochemistry of Eocene Calc-Alkaline Volcanic rocks from the Kastamonu area, Northern Turkey. *Petrology* 58, 63-81.
- [33] Shang, C. K., Liégeois, J. P., Satir, M., Frisch, W., Nsifa, E. N., 2010. Late Archean high-K granite geochronology of the northern metacratonic margin of the Archean Congo craton, Southern Cameroon: Evidence for Pb-loss due to non-metamorphic causes. *Gondwana Research* 18, pp 337-355.
- [34] Sun, S. S., et McDonough, W. F., 1989. Chemical and isotopic systematics of oceanic basalts: implications for mantle composition and processes. In: *Magmatism in the ocean basins*, SAUNDERS A. D et NORRY M. J Eds., Blackwell Sci. Publ., Oxford, p. 313-345.
- [35] Tagne-Kamga, G., 2003. Petrogenesis of neoproterozoic Ngondo plutonic complex (Cameroon West central Africa): a case of late collisional ferro-potassic magmatism. *Journal of African Earth Sciences* 36, 149-171. [https://doi.org/10.1016/S0899-5362\(03\)00043-5](https://doi.org/10.1016/S0899-5362(03)00043-5)
- [36] Tchakounté J., 1999. Etude géologique de la région d'Eoundou-Bayomen dans la série de Bafia (province du Centre): tectonique, géochimie-métamorphisme. Thèse Université Yaoundé I, 190 p.
- [37] Tchakounté Numben, J., Toteu, S. F., Van Schmus, W. R., Penaye, J., Deloule, E., Mvondo Ondoua, J., Houketchang, M. B., Ganwa, A. A., White, W. M., 2007. Evidence of ca. 1.6-Ga detrital zircon in the Bafia Group (Cameroon): Implication for the chronostratigraphy of the Pan-African Belt north of the Congo craton. *Comptes Rendus Geoscience* 339, 132-142. <https://doi.org/10.1016/j.crte.2007.01.004>
- [38] Tchakounté J. N., Eglinger, A., Toteu, S. F., Zeh, A., Nkoubou, C., Mvondo - Ondoa, J., Barbey, P., 2017. The Adamawa - Yade domain, a piece of Archean crust in the Neoproterozoic Central African Orogenic belt (Bafia area, Cameroon). *Precambrian Research* 299, 210-229. <http://dx.doi.org/10.1016/j.precamres.2017.07.001>
- [39] Tchakounté J. N., Fuh, C. G., Kamwa, A. N., Metang, V., Mvondo, O. J., Nkoubou, C., 2021. Petrology and geochemistry of the Pan-African high-K calc-alkaline to shoshonitic -adakitic Bapé plutonic suites (Adamawa-Yade block, Cameroon): evidence of a hot oceanic crust subduction. *International Journal and Earth Sciences* 110, 2067 - 2090. <https://doi.org/10.1007/s00531-021-02060-6>
- [40] Tchouankoué J. P., Simeni Wambo, N. A., Kagou Dongmo, A., Xian-Hua, Li., 2016. $^{40}\text{Ar}/^{39}\text{Ar}$ dating of basaltic dykes swarm in Western Cameroon: Evidence of Late Paleozoic and Mesozoic magmatism in the corridor of the Cameroon Line. *Journal of African Earth Sciences* 93, pp. 14-22. <https://doi.org/10.1016/j.jafrearsci.2014.01.006>
- [41] Toteu, S. F., Penaye, J., Djomani Poudjom, Y., 2004. Geodynamic evolution of the Pan-African belt in Central Africa with special reference to Cameroon. *Canadian Journal of Earth Sciences* 41, pp. 73-85. <https://doi.org/10.1139/e03-079>
- [42] Trompette, R., 1994. Geology of western Gondwana (2000-500 Ma). Pan-African-Brazilian aggregation of South America and Africa. A. A. Balkema, Rotterdam, the Netherlands: 350 p.
- [43] Toteu, S. F., Van Schmus, W. R., Penaye, J., Nyobe, J. B., 1994. U-Pb and Sm-Nd evidence for Eburnean and Pan-African high grade metamorphism in cratonic rocks of Southern Cameroon. *Precambrian Research* 67: 321-347.
- [44] Weecksteen, G., 1957. Carte géologique de reconnaissance à l'échelle du 1/500.000, territoire du Cameroun, Douala-Est. Direction des Mines et Géologie du Cameroun, Paris 1, carte et notice explicative. Imprimerie Nationale de Yaoundé 35 p.